We now postulate that $H \neq 0$, $V \neq 0$ and $v = 0$. The partial derivatives of R, U, and V are easily determined by substituting $v = 0$ in (18). Those of T are

$$\left.\begin{aligned} ET_r &= (V - G/RV)R_r + RV_r + 2G(Q - G/VE)/r^2 + GXZ_r/RVE \\ ET_u &= (V - G/RV)R_u + RV_u + 2u(Q - G/VE) + GXZ_u/RVE \\ ET_v &= (V - G/RV)R_v + RV_v - r - Gr/(G - H^2/r) \\ ET_\theta &= (V - G/RV)R_\theta + RV_\theta \end{aligned}\right\} \quad (33)$$

If both the initial and terminal states are apsides, two cases arise. If $\theta = \pi$ and $V = v = 0$

$$\left.\begin{aligned} &R_r = R^2(4G/H^2 - 1/r)/r \qquad R_u = R^2(4G/uH^2) \\ &R_v = R_\theta = 0 \qquad U_r = u/R - (4G/H - u)/r \\ &U_u = r/R - 4G/uH \qquad U_v = U_\theta = 0 \\ &V_\theta = G/H - u \qquad V_v = -1 \qquad V_u = V_r = 0 \\ &T_r = 3GT/r^2E \qquad T_\theta = R/U \\ &T_u = -3uT/E \qquad T_v = (r^2 - R^2)/(G - Hu) \end{aligned}\right\} \quad (34)$$

On the other hand, if $\theta = 2\pi$ and $V = v = 0$,

$$\begin{aligned} &R_r = U_u = V_v = 1 \qquad V_\theta = u - G/H \\ &T_r = 3GT/R^2E \qquad T_u = -3uT/E \\ &T_v = 0 \qquad T_\theta = r/u \end{aligned} \quad (35)$$

and the remaining partial derivatives are zero.

Discussion

Our representation of error in (17) is referenced to a fixed θ. If instead, we treat T as the independent variable the error coefficients can be expressed in terms of those in (17) as follows

$$\begin{bmatrix} dR \\ dU \\ dV \\ d\theta \end{bmatrix} = (M - N)\begin{bmatrix} dr \\ du \\ dv \\ dT \end{bmatrix} \qquad M = \begin{bmatrix} R_r & R_u & R_v & 0 \\ U_r & U_u & U_v & 0 \\ V_r & V_u & V_v & 0 \\ 0 & 0 & 0 & 0 \end{bmatrix}$$

$$N = \frac{1}{T_\theta}\begin{bmatrix} R_\theta T_r & R_\theta T_u & R_\theta T_v & -R_\theta \\ U_\theta T_r & U_\theta T_u & U_\theta T_v & -U_\theta \\ V_\theta T_r & V_\theta T_u & V_\theta T_v & -V_\theta \\ T_r & T_u & T_v & -1 \end{bmatrix} \quad (36)$$

We now can systematically generate errors associated with a fixed time-to-go T.

A related set of error coefficients is generated in Ref. 3. To compare the general coefficients on p. 1865 of this reference to ours in (18), it is necessary to recognize the following correspondence in notation: $r \to r_1$, $r \to R$, $u \to v_1 \cos\theta_1$, $U \to v \cos\theta$, $v \to v_1 \sin\theta_1$, $V \to v \sin\theta$, $\theta \to \eta_f$, $\alpha \to \eta_1 - \frac{1}{2}\pi$, $A \to \eta - \frac{1}{2}\pi$, $G \to K$, $Z \to K\epsilon$, $E \to K(A - 2)/r_1$.

It is evident upon comparison that the state extrapolation equations in (10) and (11) have led to a simpler set of partial derivatives. Although we must compute the invariants and the terminal variables to enjoy this simplicity, similar computations also are required to convert the normalized expressions in Ref. 3 to their useful dimensional forms. Thus the simplicity referred to is not because of notation alone.

The information contained in Eq. (A18) on p. 1865 of Ref. 3 corresponds to partial derivatives of θ in the matrix $(M-N)$ of (36). However, there is no expression in Ref. 3 equivalent to $\theta_T = -1/T_\theta$. As a consequence, this reference contains no explicit coefficients corresponding to the partial derivatives of T.

References

[1] Shapiro, I. I., *The Prediction of Ballistic Missile Trajectories from Radar Observations* (McGraw-Hill Book Co., Inc., New York, 1958).

[2] Brouwer, D. and Clemence, G. M., *Methods of Celestial Mechanics* (Academic Press Inc., New York, 1961).

[3] Gretz, R. W., "Error sensitivities in satellite ascent and orbital transfer," ARS J. **32**, 1860–1866 (1962).

Longitudinal Flow over a Circular Cylinder with Surface Mass Transfer

D. J. Wanous* and E. M. Sparrow†
University of Minnesota, Minneapolis, Minn.

Consideration is given to axisymmetric laminar boundary-layer flow longitudinal to a circular cylinder with continuously-distributed mass injection (blowing) or mass removal (suction) at the surface. Such a flow differs from that along a flat plate because of the transverse curvature of the cylindrical surface. The transverse curvature effect gives rise to nonsimilar boundary-layer solutions.

The present analysis is carried out for constant property, incompressible flow. In the case of mass addition, the properties of the injected gas are identical to those of the mainstream gas. The cylinder has a radius r_0. Radial distances are measured by r, whereas x measures axial distances downstream from the effective starting point of the boundary layer. The freestream velocity is U_∞. Solutions will be sought for two distributions of the surface mass transfer velocity: 1) $v_w \sim x^{-1/2}$, and 2) $v_w =$ const. The first of these is widely employed in mass transfer analyses, since it leads to similarity solutions for the flat-plate boundary layer. The second is of interest inasmuch as it is more easily achieved in practice. Other investigations concerned with the simultaneous effects of mass transfer and transverse curvature are reported in Refs. 1 and 2.

Analysis

1. $v_w \sim x^{-1/2}$

The analytical formulation for this case closely parallels that for the impermeable wall.[3] Upon satisfying mass conservation and transforming the momentum equation, there is obtained a partial differential equation for the dimensionless stream function f that cannot be made to yield similarity solutions. Recourse is then had to a perturbation series

$$f(\xi, \eta) = f_0(\eta) + \xi f_1(\eta) + \xi^2 f_2(\eta) + \xi^3 f_3(\eta) + \ldots \quad (1)$$

wherein

$$\begin{aligned} \xi &= (4/r_0)(\nu x/U_\infty)^{1/2} \\ \eta &= (U_\infty/\nu x)^{1/2}[(r^2 - r_0^2)/4r_0] \end{aligned} \quad (2)$$

In Ref. 3, the foregoing series was truncated at f_2, whereas in the present study terms up to and including f_3 have been retained. The ordinary differential equations governing f_0, f_1, and f_2 are stated in the reference and need not be repeated here. The f_3 equation is derived in a straightforward manner.

The essential modification in the analysis that stems from the $x^{-1/2}$ distribution of the surface mass transfer is a change in the boundary conditions. In particular, whereas formerly $f_0(0) = 0$, now $f_0(0) = F_w$, wherein

$$F_w = -2(v_w/U_\infty)(U_\infty x/\nu)^{1/2} \quad (3)$$

For the situation in which $v_w \sim x^{-1/2}$, it is evident that F_w is a constant parameter. Aside from the change in $f_0(0)$, all other boundary conditions remain unchanged. The nature of the governing equations is such that the solution for f_1 depends upon f_0, the solution for f_2 depends upon f_0 and f_1, and so forth. Thus, the fact that the f_0 function corresponding to surface mass transfer is different from the f_0 function

Received March 30, 1964; revision received August 19, 1964. This study was supported by a grant from the U. S. Air Force Office of Scientific Research, Mechanics Division.

* Research Assistant.
† Professor of Mechanical Engineering.

Table 1 Values for $f''(0)$ and $\varphi''(0)$

F_w	$f_0''(0)$	$f_1''(0)$	$f_2''(0)$	$f_3''(0)$	nk	$\varphi_{nk}''(0)$
1.0	2.91547	0.5073	−0.04599	0.01376	00	1.3282
0.7	2.41489	0.5596	−0.07055	0.02715	10	0.6943
0.5	2.09129	0.5966	−0.09125	0.04038	11	−1.2243
0.3	1.77734	0.6351	−0.1163	0.05873	20	−0.1641
0.2	1.62448	0.6548	−0.1307	0.07052	21	0.1432
0.1	1.47469	0.6745	−0.1466	0.08462	22	0.1948
0.0	1.32823	0.6943	−0.1641	0.1016	30	0.1016
−0.1	1.18540	0.7140	−0.1836	0.1222	31	−0.1321
−0.2	1.04655	0.7333	−0.2053	0.1477	32	−0.06057
−0.3	0.91205	0.7521	−0.2295	0.1797	33	0.02822
−0.5	0.65796	0.7866	−0.2880	0.2751	...	...
−0.7	0.42763	0.8134	−0.3667	0.4595	...	...
−1.0	0.14208	0.8173	−0.5873	1.644	...	...

for the impermeable surface implies the same state of affairs for the functions $f_1, f_2, \ldots$.

The standard definitions of the friction coefficient c_f and the Reynolds number Re_x can be employed to achieve a dimensionless representation of the local wall shear τ; thus

$$c_f = \tau/\tfrac{1}{2}\rho U_\infty^2 \qquad Re_x = U_\infty x/\nu \tag{4}$$

In terms of these, one finds

$$2c_f Re_x^{1/2} = f_0''(0) + \xi f_1''(0) + \xi^2 f_2''(0) + \xi^3 f_3''(0) \tag{5a}$$

$$[2c_f Re_x^{1/2}]_{fp} = f_0''(0) \tag{5b}$$

in which the subscript fp denotes the flat-plate case. Numerical values of the $f''(0)$ are listed in Table 1 and will be utilized in the forthcoming presentation of results.

2. $v_w = const$

The case of uniformly distributed surface mass transfer is analytically more interesting than the $x^{-1/2}$ distribution. Indeed, for uniform mass transfer, similarity-type solutions cannot even be found for the flat-plate boundary layer. The analysis is facilitated by defining the stream function ψ as

$$\psi = r_0(\nu x U_\infty)^{1/2}\varphi(\xi, \eta) - v_w r_0 x \tag{6}$$

wherein φ represents a dimensionless stream function, and (ξ, η) are given by Eq. (2). The partial differential equation for φ, derived by introducing ψ, ξ, and η into the momentum equation, is solved by a perturbation series where, in turn,

$$\varphi(\xi, \eta) = \varphi_0(\eta) + \xi\varphi_1(\eta) + \xi^2\varphi_2(\eta) + \xi^3\varphi_3(\eta) + \ldots \tag{7a}$$

$$\varphi_n(\eta) = \sum_{k=0}^{n} \left(\frac{v_w r_0}{2\nu}\right)^k \varphi_{nk}(\eta) \tag{7b}$$

The $\varphi_{nk}(\eta)$ are universal functions, that is, they are independent of any parameters. The ordinary differential equations governing the φ_{nk} and the corresponding boundary conditions cannot be stated here because of space limitations; however, they are given in detail in Ref. 4.

The local skin friction can be evaluated from the definition of ψ [Eq. (6)] and then rephrased as follows:

$$\begin{aligned}2c_f Re_x^{1/2} = {} & \varphi_{00}''(0) + [\xi\varphi_{10}''(0) - F_w\varphi_{11}''(0)] + \\ & [\xi^2\varphi_{20}''(0) - \xi F_w\varphi_{21}''(0) + F_w^2\varphi_{22}''(0)] + \\ & [\xi^3\varphi_{30}''(0) - \xi^2 F_w\varphi_{31}''(0) + \\ & \xi F_w^2\varphi_{32}''(0) - F_w^3\varphi_{33}''(0)]\end{aligned} \tag{8a}$$

Correspondingly, for the flat plate ($\xi = 0$),

$$[2c_f Re_x^{1/2}]_{fp} = \varphi_{00}''(0) - F_w\varphi_{11}''(0) + F_w^2\varphi_{22}''(0) - F_w^3\varphi_{33}''(0) \tag{8b}$$

In the rearrangement leading to Eqs. (8a) and (8b), the identity $(v_w r_0/2\nu) = -F_w/\xi$ has been employed. Inspection of Eq. (8a) reveals a double perturbation due to transverse curvature (parameter ξ) and nonsimilar mass transfer (parameter F_w). The first bracket on the right contains the first-order perturbation, the second bracket contains the second-order perturbation, and so forth. Values of the $\varphi_{nk}''(0)$ are given in Table 1 and will be applied in the next section of the report.

Results

A graphical presentation of the local skin-friction results is made in Fig. 1, the left- and right-hand portions of which pertain, respectively, to $v_w \sim x^{-1/2}$ and v_w = const. The ordinate is the ratio of $c_f\, Re_x^{1/2}$ for the cylinder to $c_f\, Re_x^{1/2}$ for the flat plate; thus, the departure of the curves from unity is an immediate measure of the effect of transverse curvature. The abscissa is the transverse curvature parameter ξ, increasing values of which imply an increase in the boundary-layer thickness relative to the cylinder radius r_0. The curves are labeled according to the surface mass-transfer parameter F_w, positive values of which indicate suction and negative values of which indicate blowing. Moreover, each curve is also labeled with the flat plate value of $c_f\, Re_x^{1/2}$ corresponding to the specified F_w.

From the figure, it is seen that the skin-friction coefficient for the cylinder is always greater than that for the flat plate; the deviations becoming more marked as the boundary-layer thickness grows larger relative to the cylinder radius (i.e., larger ξ). Blowing ($F_w < 0$) tends to accentuate the effect of transverse curvature, whereas suction ($F_w > 0$) tends to diminish the curvature effect. This is because blowing thickens the boundary layer, whereas suction thins the boundary layer.

The preceding figure was intended to highlight the effect of transverse curvature. Consideration will now be given to the lower portion of Fig. 2, which illuminates the effect of surface mass transfer. The ordinate is the ratio of $c_f\, Re_x^{1/2}$ for surface mass transfer to $c_f\, Re_x^{1/2}$ for the impermeable wall; thus, the departure of the curves from unity is a direct measure of the effect of mass transfer. The abscissa is the mass

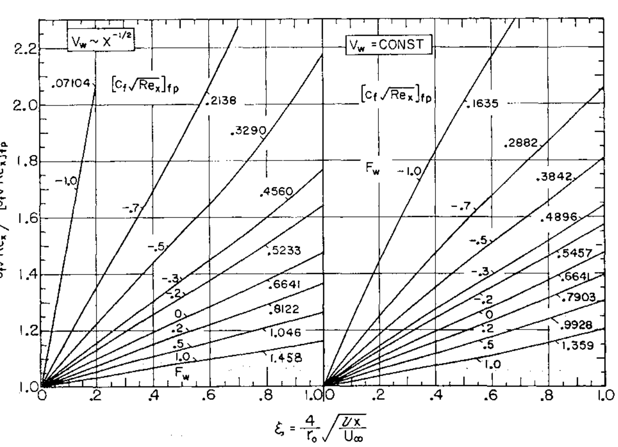

Fig. 1 Effect of transverse curvature on skin friction.

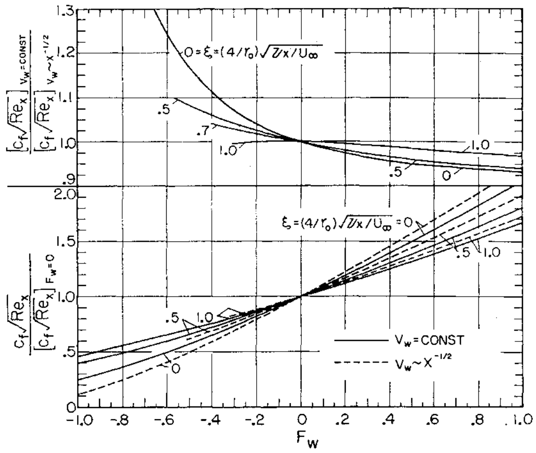

Fig. 2 Effect of surface mass transfer on skin friction.

transfer parameter F_w, and the curves are parameterized by ξ. The case $\xi = 0$ corresponds to the flat plate. By inspecting the figure, one sees that the general effect of blowing ($F_w < 0$) is to decrease the skin friction, whereas suction ($F_w > 0$) increases the skin friction. Further study shows that, for a given value of the F_w parameter, the effect of surface mass transfer is diminished as ξ increases. Thus, the flat plate is most affected by surface mass transfer and cylinders ($r_0 < \infty$) are affected to a lesser extent.

The essential point of this finding is that surface mass transfer and transverse curvature oppose one another. In the case of blowing, the boundary layer is thickened and the skin friction is reduced; however, the thickening of the boundary layer accentuates the transverse curvature effect, which in turn tends to increase the skin friction. The net effect is a reduction in skin friction, but to an extent that is less than that for the flat plate.

Next, attention may be directed to a comparison of results for the two distributions of surface mass transfer as shown in the upper portion of Fig. 2. The ordinate is the ratio of $c_f\, Re_x^{1/2}$ for uniform mass transfer to $c_f\, Re_x^{1/2}$ for the $v_w \sim x^{-1/2}$ mass-transfer distribution. In general, it appears that the $x^{-1/2}$ distribution is somewhat more effective in increasing skin friction by suction and decreasing skin friction by blowing than is the uniform distribution. However, aside from the flat plate with blowing, the results are remarkably insensitive to the detailed distribution of the surface mass transfer.

Numerical values of the displacement thickness cannot be reported here because of space limitations, but these are available in Ref. 4. As a final remark, it is of interest to note that the present investigation extends the range of results for uniform blowing for the flat plate. Previous information, obtained by a finite-difference solution[5] was restricted to $F_w = -0.141$ and -0.283.

References

[1] Lew, H. G., "The asymptotic behavior of the boundary layer to transverse curvature," J. Aeronaut. Sci. **23**, 276–277, 895–897 (1956).

[2] Steiger, M. H. and Bloom, M. H., "On thick boundary layers over slender bodies with some effects of heat transfer, mass transfer, and pressure gradient," Intern. J. Heat Mass Transfer **5**, 513–520 (1962).

[3] Seban, R. A. and Bond, R., "Skin friction and heat transfer characteristics of a laminar boundary layer on a cylinder in axial incompressible flow," J. Aeronaut. Sci. **18**, 671–675 (1951).

[4] Wanous, D. J., "Heat transfer and skin friction for longitudinal flow over a cylinder with surface mass transfer," M.S. Thesis, Dept. of Mechanical Engineering, Univ. of Minnesota (1963).

[5] Lew, H. G. and Fanucci, J. B., "On the compressible boundary layer over a flat plate with suction and injection, J. Aeronaut. Sci. **22**, 589–597 (1955).

A Practical Note on the Use of Lambert's Equation

Geza S. Gedeon*
Northrop Space Laboratories, Hawthorne, Calif.

Nomenclature

μ $\cong GM$ product of universal gravitational constant and mass of principal attracting body
e = eccentricity
a = semimajor axis
r = separation from the dynamical center
c = chord
s = $(r_0 + r + c)/2$ = semiperimeter
z = $s/2a$ = argument of the Lambertian series
w = $(1 - c/s)^{1/2}$ = shape factor
n_s = $(\mu/s^3)^{1/2}$ = mean motion based on semiperimeter
A_n = $\dfrac{1\cdot3\cdot5\ldots(2n-1)}{2\cdot4\cdot6\ldots(2n)}$; $A_0 = 1$
N = $n_s t$ = mean anomaly based on semiperimeter
α, β = Lambert's angles for elliptic orbits
γ, δ = Lambert's angles for hyperbolic orbits
k = ±1
m = 1, 2 . . . integer

When the time of flight is given between two terminals, the equations of Lambert are used to determine the orbit. These equations, however, have several drawbacks, and the following will show how to overcome these difficulties without compromising the simplicity of the original expressions.

Lambert's equations are the following:

Hyperbolic Orbits

$$t = (|a|^3/\mu)^{1/2}[(\sinh\gamma - \gamma) - (\sinh\delta - \delta)] \qquad (1)$$

$$\sinh(\gamma/2) = (s/2|a|)^{1/2}$$
$$\sinh(\delta/2) = [(s - c)/2|a|]^{1/2} \qquad (2)$$

Parabolic Orbits

$$t = \tfrac{1}{3}(2/\mu)^{1/2}[s^{3/2} \mp (s - c)^{3/2}] \qquad (3)$$

Elliptic Orbits

$$t = (a^3/\mu)^{1/2}[(1 - k)m\pi + k(\alpha - \sin\alpha) \mp (\beta - \sin\beta)] \qquad (4)$$

$$\sin\frac{\alpha}{2} = \left(\frac{s}{2a}\right)^{1/2} \qquad \sin\frac{\beta}{2} = \left(\frac{s - c}{2a}\right)^{1/2} \qquad (5)$$

where $k = \pm1$ and $m = 1, 2\ldots$ integer number of loops (see, e.g., Ref. 1).

To solve these equations for a on an automatic digital computer, the fast and efficient Newton-Raphson method can be applied if the derivatives are available. To obtain these derivatives, the auxiliary equations (2) and (5) will be eliminated by the introduction of the variable

$$z = s/2a \qquad (6)$$

and the constants

$$w = \pm(1 - c/s)^{1/2} \qquad n_s = (\mu^3/s)^{1/2} \qquad (7)$$

With these substitutions, Eqs. (1) and (4) and their derivatives can be written in the combined form

$$N = n_s t = \frac{1}{z|z|^{1/2}\,2^{1/2}}\left\{\frac{1-k}{2}\,m\pi + k[f(|z|^{1/2}) - |z|^{1/2}(1 - z)^{1/2}] - [f(w|z|^{1/2}) - w|z|^{1/2}(1 - w^2 z)^{1/2}]\right\} \qquad (8a)$$

Received April 6, 1964; revision received August 21, 1964.

* Chief, Flight Mechanics Group. Associate Fellow Member AIAA.